Extended Abstracts of the 2016 International Conference on Solid State Devices and Materials, Tsukuba, 2016, pp575-576

N-3-02

Terahertz Detector Using High Electron Mobility Transistor with Reduced Series Resistance for High Responsivity

Satoshi Shibuya, Yuki Isobe, and Safumi Suzuki

Department of Electrical and Electronic Engineering, Tokyo Institute of Technology
2-12-1-S3-35 O-okayama, Meguro-ku, Tokyo 101-0024, Japan
Phone: +81-3-5734-3039 E-mail: safumi@ee.e.titech.ac.jp

Abstract

A high-responsivity terahertz (THz) detector was fabricated using an InAlAs/InGaAs high-electron-mobility-transistor (HEMT) integrated with bow-tie antenna. We employed a high-indium content and thick contact layer for reduction in series resistance, and obtained a maximum transconductance of 1.6 S/mm and the subthreshold slope of 80 mV/dec in 50-nm-long gate. The measured current sensitivity and noise equivalent power were 5.8 A/W and 0.7 pW/Hz$^{1/2}$, respectively.

1. Introduction

The terahertz (THz) frequency range located between the lightwave and millimeter wave has been receiving considerable attention because of its many possible applications, such as imaging, spectroscopy, and high-capacity wireless communications [1]. Compact, high responsivity, and low noise detectors are key components for various applications of the THz waves. Conventional Schottky barrier diode (SBD) detectors have been used for various terahertz applications. However, current responsivity R_i decreases in high-frequency operation because the area of the Schottky junction is small, as required for increasing the cutoff frequency. Recently, detectors using field effect transistors have been studied intensively [2-5]. In contrast with the SBD detector, the cutoff frequency of a HEMT detector can be increased by reduction in the gate length without reducing R_i. We proposed and fabricated a THz detector using an InGaAs composite-channel HEMT with maximum transconductance $g_{m.max}$ of 1.2 S/mm, and achieved high R_i (5 A/W) [6]. Because, R_i is proportion to $g_{m.max}$, increase in $g_{m.max}$ by reduction in series resistance is effective for high responsivity.

In this study, we employed a high-indium content and thick contact layer for reduction in series resistance. We achieved increment in $g_{m.max}$ (1.6 S/mm) and higher current responsivity of 5.8 A/W. A noise characteristics was also measured, and a low noise equivalent power (NEP) of 0.7 pW/Hz$^{1/2}$ was obtained.

2. Device Structure and Detection Mechanism

The schematic device structure of our HEMT THz detector is shown in Fig. 1. An InP-based InAlAs/InGaAs composite-channel HEMT with two-finger T-shaped gates was integrated at the center of a bow-tie antenna. A Pt-buried gate process was used to reduce the short channel effect for small *S.S.* value [7]. The metal–insulator–metal (MIM) capacitor was connected between the gate and the drain; it was shorted in the THz frequency and open for the direct current to provide a bias voltage.

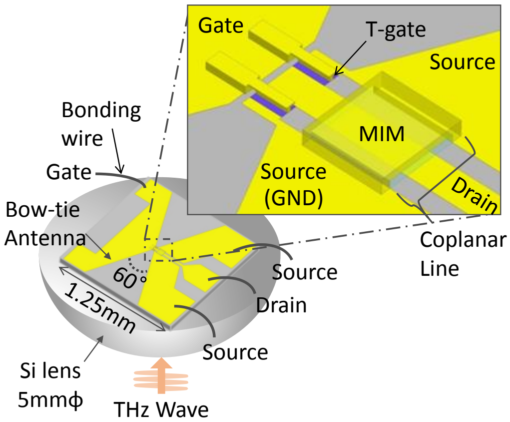

Fig. 1 Schematic of the HEMT THz detector structure integrated with bow-tie antenna. The antenna impedance R_a of a bow-tie antenna with an angle of 60° was 50 Ω.

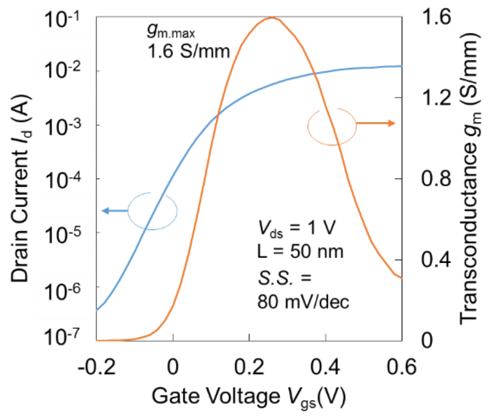

Fig. 2 I_d-V_{gs} and transconductance characteristics. Low subthreshold slope was obtained with Pt-buried gate.

Because, the FET has diode-like characteristics in the I_d–V_{gs} characteristics, irradiated THz wave can be detected by rectification. Although the detection mechanism is basically the same as that used for non-resonant plasmonic detection [2, 3], a high current responsivity is expected, owing to ballistic transport in the short-gate HEMT [6]. Using $g_{m.max}$ and subthreshold slope *S.S.*, R_i is roughly expressed as $R_i \approx g_{m.max} \cdot WR_a/S.S.$, where R_a is antenna impedance and W is gate width

[6]. A high value of $g_{m.max}$ with small subthreshold characteristics is required for high responsivity. The voltage responsivity R_v is given by $R_i \times R_d$, where R_d is drain resistance.

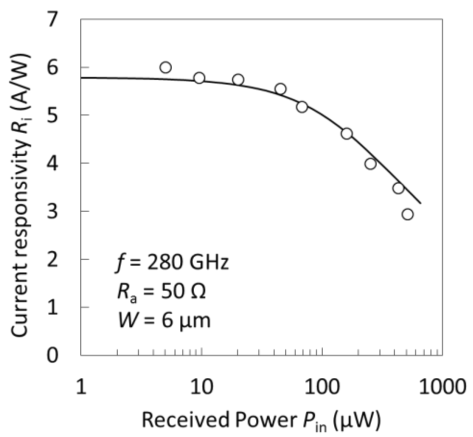

Fig. 3 Dependence of current responsivity R_i on received power P_{in}.

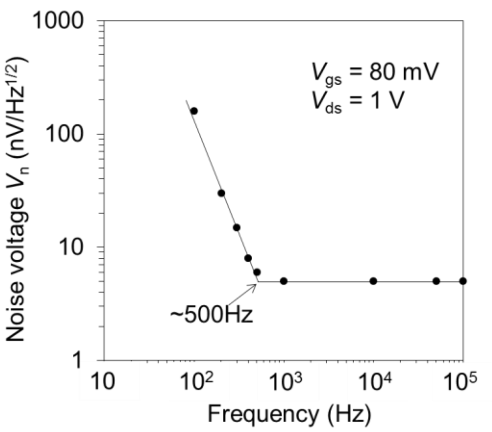

Fig. 4 Frequency dependence of noise voltage.

The epitaxial layer structure was grown by molecular beam epitaxy on semi-insulating (100) InP substrates. From bottom to top, the layers consist of a 200-nm InAlAs buffer, a 10-nm InGaAs composite-channel, a 3-nm InAlAs spacer, a Si δ-doping of 5×10^{12} cm^{-2}, a 2-nm InAlAs barrier, a 3-nm InP etching-stopper, a 10-nm layer of n^+-InAlAs (3×10^{19} cm^{-3}), a 40 nm n^+-InGaAs contact layer (5×10^{19} cm^{-3}) , and a 9 nm high-indium-content n^+-InGaAs top contact layer (5×10^{19} cm^{-3}). Compared to the previous structure [6], we employed thick contact layer (from 15 nm to 40 nm) and high-indium-content n^+-InGaAs top contact layer. By these improvements, we obtained reduction in contact resistance from 0.054 to 0.023 Ωmm and sheet resistance from 65 to 27 Ω/□. The measured I_d-V_{gs} and transconductace characteristics were shown in Fig. 2. We obtained higher $g_{m.max}$ (1.6 S/mm) by the reduction in series resistance. The measured *S.S.* value was 80 mV/dec.

The current responsivity R_i, measured as a function of the received power of 280 GHz signal, is shown in Fig. 5b. A maximum R_i of 5.8 A/W was obtained in the low-received-power region. The R_i drops with received power because of the degradation of nonlinearity in case of large signal. We obtained higher R_i owing to higher $g_{m.max}$. Using measured R_d of 1.2 kΩ, R_v was simply obtained as 7 kV/W.

We also measured the noise characteristics of the HEMT detector. The frequency dependence of noise voltage V_n is shown in Fig. 4. The 1/f noise decreases with frequency, and V_n became flat above the 1/f corner frequency of ~500 Hz. V_n of 5 nV/Hz$^{1/2}$ was obtained above ~500 Hz, which is well agreed with the theoretical thermal noise of 4.5 nV/Hz$^{1/2}$ generated by 1.2 kΩ drain resistance. Because HEMT detector is operated in subthreshold region, the channel thermal noise is small and the thermal noise due to drain resistance is dominant. Using R_v of 7 kV/W and V_n of 5 nV/Hz$^{1/2}$, NEP (= V_n/R_v) was obtained as ~0.7 pW/Hz$^{1/2}$. We achieved very low NEP value with high responsivity HEMT THz detector. Lower NEP can be realized using a state-of-the-art HEMT having very high g_{mmax} of 3.1 S/mm [8].

3. Conclusions

A high-responsivity THz detector was fabricated using an InAlAs/InGaAs HEMT integrated with bow-tie antenna. We employed a high-indium content and thick contact layer for reduction in series resistance, and obtained a maximum transconductance of 1.6 S/mm and the subthreshold slope of 80 mV/dec in 50-nm-long gate. The measured current sensitivity and noise equivalent power were 5.8 A/W and 0.7 pW/Hz$^{1/2}$, respectively.

Acknowledgements

The authors thank Emeritus Professors Y. Suematsu and K. Furuya of the Tokyo Institute of Technology for their continuous encouragement. We also thank Professors S. Arai and Y. Miyamoto and Associate Professors M. Watanabe and N. Nishiyama of the Tokyo Institute of Technology for fruitful discussions and encouragement. This work was supported by Scientific Grants-in-Aid from the Ministry of Education, Culture, Sports, Science and Technology, Japan; the Industry–Academia Collaborative R&D Program from the Japan Science and Technology Agency, Japan; and the Strategic Information and Communications R&D Promotion Programme (SCOPE) from the Ministry of Internal Affairs and Communications.

References

[1] M. Tonouchi, Nat. Photonics **1** (2007) 97.

[2] T. Watanabe, S. B. Tombet, Y. Tanimoto, Y. Wang, H. Minamide, H. Ito, D. Fateev, V. Popov, D. Coquillat, W. Knap, Y. Meziani, T. Otsuji, Solid-State Electron. **78** (2012) 109.

[3] W. Knap, V. Kachorovskii, Y. Deng, S. Rumyantsev, J.-Q. Lü, R. Gaska, M. S. Shur, G. Simin, X. Hu, M. Asif Khan, C. A. Saylor, L. C. Brunel, J. Appl. Phys. **91** (2002) 9346.

[4] E. Ojefors, A. Lisauskas, D. Glaab, H. G. Roskos, U. R. Pfeiffer, J. Infrared Milli. Terahertz Waves **30** 1269 (2009)

[5] M. Sakhno, F. Sizov, A. Golenkov, J. Infrared Milli. Terahertz Waves **34** (2013) 798.

[6] S. Suzuki, T. Nukariya, Y. Ueda, T. Otsuka, and M. Asada, J. Infrared Milli. Terahertz Waves, Online First, (DOI 10.1007/s10762-016-0260-2).

[7] S. H. Shin, T.-W. Kim, J.-I. Song, J.-H. Jang, Solid-State Electron. **62** (2011) 106.

[8] X. Mei, W. Yoshida, M. Lange, J. Lee, J. Zhou, P. Liu, K. Leong, A. Zamora, J. Padilla, S. Sarkozy, R. Lai, and W. R. Deal, IEEE Electron. Device Lett. **36** (2015) 327.